UC Berkeley
UC Berkeley Previously Published Works

Title

Search for b→u transitions in B0→D0K*0 decays

Permalink

https://escholarship.org/uc/item/5d98b1vr

Journal

Physical Review D, 80(3)

ISSN

2470-0010

Authors

Aubert, B
Bona, M
Karyotakis, Y
et al.

Publication Date

2009-08-01

DOI

10.1103/physrevd.80.031102

Peer reviewed

Search for $b \to u$ transitions in $B^0 \to D^0 K^{*0}$ decays

B. Aubert,[1] M. Bona,[1] Y. Karyotakis,[1] J. P. Lees,[1] V. Poireau,[1] E. Prencipe,[1] X. Prudent,[1] V. Tisserand,[1] J. Garra Tico,[2] E. Grauges,[2] L. Lopez,[3a,3b] A. Palano,[3a,3b] M. Pappagallo,[3a,3b] G. Eigen,[4] B. Stugu,[4] L. Sun,[4] G. S. Abrams,[5] M. Battaglia,[5] D. N. Brown,[5] R. N. Cahn,[5] R. G. Jacobsen,[5] L. T. Kerth,[5] Yu. G. Kolomensky,[5] G. Lynch,[5] I. L. Osipenkov,[5] M. T. Ronan,[5,*] K. Tackmann,[5] T. Tanabe,[5] C. M. Hawkes,[6] N. Soni,[6] A. T. Watson,[6] H. Koch,[7] T. Schroeder,[7] D. Walker,[8] D. J. Asgeirsson,[9] B. G. Fulsom,[9] C. Hearty,[9] T. S. Mattison,[9] J. A. McKenna,[9] M. Barrett,[10] A. Khan,[10] V. E. Blinov,[11] A. D. Bukin,[11] A. R. Buzykaev,[11] V. P. Druzhinin,[11] V. B. Golubev,[11] A. P. Onuchin,[11] S. I. Serednyakov,[11] Yu. I. Skovpen,[11] E. P. Solodov,[11] K. Yu. Todyshev,[11] M. Bondioli,[12] S. Curry,[12] I. Eschrich,[12] D. Kirkby,[12] A. J. Lankford,[12] P. Lund,[12] M. Mandelkern,[12] E. C. Martin,[12] D. P. Stoker,[12] S. Abachi,[13] C. Buchanan,[13] J. W. Gary,[14] F. Liu,[14] O. Long,[14] B. C. Shen,[14,*] G. M. Vitug,[14] Z. Yasin,[14] L. Zhang,[14] V. Sharma,[15] C. Campagnari,[16] T. M. Hong,[16] D. Kovalskyi,[16] M. A. Mazur,[16] J. D. Richman,[16] T. W. Beck,[17] A. M. Eisner,[17] C. J. Flacco,[17] C. A. Heusch,[17] J. Kroseberg,[17] W. S. Lockman,[17] A. J. Martinez,[17] T. Schalk,[17] B. A. Schumm,[17] A. Seiden,[17] M. G. Wilson,[17] L. O. Winstrom,[17] C. H. Cheng,[18] D. A. Doll,[18] B. Echenard,[18] F. Fang,[18] D. G. Hitlin,[18] I. Narsky,[18] T. Piatenko,[18] F. C. Porter,[18] R. Andreassen,[19] G. Mancinelli,[19] B. T. Meadows,[19] K. Mishra,[19] M. D. Sokoloff,[19] P. C. Bloom,[20] W. T. Ford,[20] A. Gaz,[20] J. F. Hirschauer,[20] M. Nagel,[20] U. Nauenberg,[20] J. G. Smith,[20] K. A. Ulmer,[20] S. R. Wagner,[20] R. Ayad,[21,†] A. Soffer,[21,‡] W. H. Toki,[21] R. J. Wilson,[21] D. D. Altenburg,[22] E. Feltresi,[22] A. Hauke,[22] H. Jasper,[22] M. Karbach,[22] J. Merkel,[22] A. Petzold,[22] B. Spaan,[22] K. Wacker,[22] M. J. Kobel,[23] W. F. Mader,[23] R. Nogowski,[23] K. R. Schubert,[23] R. Schwierz,[23] A. Volk,[23] D. Bernard,[24] G. R. Bonneaud,[24] E. Latour,[24] M. Verderi,[24] P. J. Clark,[25] S. Playfer,[25] J. E. Watson,[25] M. Andreotti,[26a,26b] D. Bettoni,[26a] C. Bozzi,[26a] R. Calabrese,[26a,26b] A. Cecchi,[26a,26b] G. Cibinetto,[26a,26b] P. Franchini,[26a,26b] E. Luppi,[26a,26b] M. Negrini,[26a,26b] A. Petrella,[26a,26b] L. Piemontese,[26a] V. Santoro,[26a,26b] R. Baldini-Ferroli,[27] A. Calcaterra,[27] R. de Sangro,[27] G. Finocchiaro,[27] S. Pacetti,[27] P. Patteri,[27] I. M. Peruzzi,[27,§] M. Piccolo,[27] M. Rama,[27] A. Zallo,[27] A. Buzzo,[28a,28b] R. Contri,[28a,28b] M. Lo Vetere,[28a,28b] M. M. Macri,[28a] M. R. Monge,[28a,28b] S. Passaggio,[28a] C. Patrignani,[28a,28b] E. Robutti,[28a] A. Santroni,[28a,28b] S. Tosi,[28a,28b] K. S. Chaisanguanthum,[29] M. Morii,[29] A. Adametz,[30] J. Marks,[30] S. Schenk,[30] U. Uwer,[30] V. Klose,[31] H. M. Lacker,[31] D. J. Bard,[32] P. D. Dauncey,[32] J. A. Nash,[32] M. Tibbetts,[32] P. K. Behera,[33] X. Chai,[33] M. J. Charles,[33] U. Mallik,[33] J. Cochran,[34] H. B. Crawley,[34] L. Dong,[34] W. T. Meyer,[34] S. Prell,[34] E. I. Rosenberg,[34] A. E. Rubin,[34] Y. Y. Gao,[35] A. V. Gritsan,[35] Z. J. Guo,[35] C. K. Lae,[35] N. Arnaud,[36] J. Béquilleux,[36] A. D'Orazio,[36] M. Davier,[36] J. Firmino da Costa,[36] G. Grosdidier,[36] A. Höcker,[36] V. Lepeltier,[36] F. Le Diberder,[36] A. M. Lutz,[36] S. Pruvot,[36] P. Roudeau,[36] M. H. Schune,[36] J. Serrano,[36] V. Sordini,[36,‖] A. Stocchi,[36] G. Wormser,[36] D. J. Lange,[37] D. M. Wright,[37] I. Bingham,[38] J. P. Burke,[38] C. A. Chavez,[38] J. R. Fry,[38] E. Gabathuler,[38] R. Gamet,[38] D. E. Hutchcroft,[38] D. J. Payne,[38] C. Touramanis,[38] A. J. Bevan,[39] C. K. Clarke,[39] K. A. George,[39] F. Di Lodovico,[39] R. Sacco,[39] M. Sigamani,[39] G. Cowan,[40] H. U. Flaecher,[40] D. A. Hopkins,[40] S. Paramesvaran,[40] F. Salvatore,[40] A. C. Wren,[40] D. N. Brown,[41] C. L. Davis,[41] A. G. Denig,[42] M. Fritsch,[42] W. Gradl,[42] G. Schott,[42] K. E. Alwyn,[43] D. Bailey,[43] R. J. Barlow,[43] Y. M. Chia,[43] C. L. Edgar,[43] G. Jackson,[43] G. D. Lafferty,[43] T. J. West,[43] J. I. Yi,[43] J. Anderson,[44] C. Chen,[44] A. Jawahery,[44] D. A. Roberts,[44] G. Simi,[44] J. M. Tuggle,[44] C. Dallapiccola,[45] X. Li,[45] E. Salvati,[45] S. Saremi,[45] R. Cowan,[46] D. Dujmic,[46] P. H. Fisher,[46] G. Sciolla,[46] M. Spitznagel,[46] F. Taylor,[46] R. K. Yamamoto,[46] M. Zhao,[46] P. M. Patel,[47] S. H. Robertson,[47] A. Lazzaro,[48a,48b] V. Lombardo,[48a] F. Palombo,[48a,48b] J. M. Bauer,[49] L. Cremaldi,[49] R. Godang,[49,¶] R. Kroeger,[49] D. A. Sanders,[49] D. J. Summers,[49] H. W. Zhao,[49] M. Simard,[50] P. Taras,[50] F. B. Viaud,[50] H. Nicholson,[51] G. De Nardo,[52a,52b] L. Lista,[52a] D. Monorchio,[52a,52b] G. Onorato,[52a,52b] C. Sciacca,[52a,52b] G. Raven,[53] H. L. Snoek,[53] C. P. Jessop,[54] K. J. Knoepfel,[54] J. M. LoSecco,[54] W. F. Wang,[54] G. Benelli,[55] L. A. Corwin,[55] K. Honscheid,[55] H. Kagan,[55] R. Kass,[55] J. P. Morris,[55] A. M. Rahimi,[55] J. J. Regensburger,[55] S. J. Sekula,[55] Q. K. Wong,[55] N. L. Blount,[56] J. Brau,[56] R. Frey,[56] O. Igonkina,[56] J. A. Kolb,[56] M. Lu,[56] R. Rahmat,[56] N. B. Sinev,[56] D. Strom,[56] J. Strube,[56] E. Torrence,[56] G. Castelli,[57a,57b] N. Gagliardi,[57a,57b] M. Margoni,[57a,57b] M. Morandin,[57a] M. Posocco,[57a] M. Rotondo,[57a] F. Simonetto,[57a,57b] R. Stroili,[57a,57b] C. Voci,[57a,57b] P. del Amo Sanchez,[58] E. Ben-Haim,[58] H. Briand,[58] G. Calderini,[58] J. Chauveau,[58] P. David,[58] L. Del Buono,[58] O. Hamon,[58] Ph. Leruste,[58] J. Ocariz,[58] A. Perez,[58] J. Prendki,[58] S. Sitt,[58] L. Gladney,[59] M. Biasini,[60a,60b] R. Covarelli,[60a,60b] E. Manoni,[60a,60b] C. Angelini,[61a,61b] G. Batignani,[61a,61b] S. Bettarini,[61a,61b] M. Carpinelli,[61a,61b,**] A. Cervelli,[61a,61b] F. Forti,[61a,61b] M. A. Giorgi,[61a,61b] A. Lusiani,[61a,61c] G. Marchiori,[61a,61b] M. Morganti,[61a,61b] N. Neri,[61a,61b] E. Paoloni,[61a,61b] G. Rizzo,[61a,61b] J. J. Walsh,[61a] D. Lopes Pegna,[62] C. Lu,[62] J. Olsen,[62] A. J. S. Smith,[62] A. V. Telnov,[62] F. Anulli,[63a] E. Baracchini,[63a,63b] G. Cavoto,[63a] D. del Re,[63a,63b] E. Di Marco,[63a,63b] R. Faccini,[63a,63b] F. Ferrarotto,[63a] F. Ferroni,[63a,63b] M. Gaspero,[63a,63b] P. D. Jackson,[63a] L. Li Gioi,[63a] M. A. Mazzoni,[63a] S. Morganti,[63a]

G. Piredda,[63a] F. Polci,[63a,63b] F. Renga,[63a,63b] C. Voena,[63a] M. Ebert,[64] T. Hartmann,[64] H. Schröder,[64] R. Waldi,[64] T. Adye,[65] B. Franek,[65] E. O. Olaiya,[65] F. F. Wilson,[65] S. Emery,[66] M. Escalier,[66] L. Esteve,[66] S. F. Ganzhur,[66] G. Hamel de Monchenault,[66] W. Kozanecki,[66] G. Vasseur,[66] Ch. Yèche,[66] M. Zito,[66] X. R. Chen,[67] H. Liu,[67] W. Park,[67] M. V. Purohit,[67] R. M. White,[67] J. R. Wilson,[67] M. T. Allen,[68] D. Aston,[68] R. Bartoldus,[68] P. Bechtle,[68] J. F. Benitez,[68] R. Cenci,[68] J. P. Coleman,[68] M. R. Convery,[68] J. C. Dingfelder,[68] J. Dorfan,[68] G. P. Dubois-Felsmann,[68] W. Dunwoodie,[68] R. C. Field,[68] A. M. Gabareen,[68] S. J. Gowdy,[68] M. T. Graham,[68] P. Grenier,[68] C. Hast,[68] W. R. Innes,[68] J. Kaminski,[68] M. H. Kelsey,[68] H. Kim,[68] P. Kim,[68] M. L. Kocian,[68] D. W. G. S. Leith,[68] S. Li,[68] B. Lindquist,[68] S. Luitz,[68] V. Luth,[68] H. L. Lynch,[68] D. B. MacFarlane,[68] H. Marsiske,[68] R. Messner,[68] D. R. Muller,[68] H. Neal,[68] S. Nelson,[68] C. P. O'Grady,[68] I. Ofte,[68] A. Perazzo,[68] M. Perl,[68] B. N. Ratcliff,[68] A. Roodman,[68] A. A. Salnikov,[68] R. H. Schindler,[68] J. Schwiening,[68] A. Snyder,[68] D. Su,[68] M. K. Sullivan,[68] K. Suzuki,[68] S. K. Swain,[68] J. M. Thompson,[68] J. Va'vra,[68] A. P. Wagner,[68] M. Weaver,[68] C. A. West,[68] W. J. Wisniewski,[68] M. Wittgen,[68] D. H. Wright,[68] H. W. Wulsin,[68] A. K. Yarritu,[68] K. Yi,[68] C. C. Young,[68] V. Ziegler,[68] P. R. Burchat,[69] A. J. Edwards,[69] S. A. Majewski,[69] T. S. Miyashita,[69] B. A. Petersen,[69] L. Wilden,[69] S. Ahmed,[70] M. S. Alam,[70] J. A. Ernst,[70] B. Pan,[70] M. A. Saeed,[70] S. B. Zain,[70] S. M. Spanier,[71] B. J. Wogsland,[71] R. Eckmann,[72] J. L. Ritchie,[72] A. M. Ruland,[72] C. J. Schilling,[72] R. F. Schwitters,[72] B. W. Drummond,[73] J. M. Izen,[73] X. C. Lou,[73] F. Bianchi,[74a,74b] D. Gamba,[74a,74b] M. Pelliccioni,[74a,74b] M. Bomben,[75a,75b] L. Bosisio,[75a,75b] C. Cartaro,[75a,75b] G. Della Ricca,[75a,75b] L. Lanceri,[75a,75b] L. Vitale,[75a,75b] V. Azzolini,[76] N. Lopez-March,[76] F. Martinez-Vidal,[76] D. A. Milanes,[76] A. Oyanguren,[76] J. Albert,[76] Sw. Banerjee,[76] B. Bhuyan,[76] H. H. F. Choi,[76] K. Hamano,[76] R. Kowalewski,[76] M. J. Lewczuk,[76] I. M. Nugent,[76] J. M. Roney,[76] R. J. Sobie,[76] T. J. Gershon,[77] P. F. Harrison,[77] J. Ilic,[77] T. E. Latham,[77] G. B. Mohanty,[77] H. R. Band,[78] X. Chen,[78] S. Dasu,[78] K. T. Flood,[78] Y. Pan,[78] M. Pierini,[79] R. Prepost,[79] C. O. Vuosalo,[79] and S. L. Wu[79]

(*BABAR* Collaboration)

[1]*Laboratoire de Physique des Particules, IN2P3/CNRS et Université de Savoie, F-74941 Annecy-Le-Vieux, France*
[2]*Universitat de Barcelona, Facultat de Fisica, Departament ECM, E-08028 Barcelona, Spain*
[3a]*INFN Sezione di Bari, I-70126 Bari, Italy*
[3b]*Dipartmento di Fisica, Università di Bari, I-70126 Bari, Italy*
[4]*University of Bergen, Institute of Physics, N-5007 Bergen, Norway*
[5]*Lawrence Berkeley National Laboratory and University of California, Berkeley, California 94720, USA*
[6]*University of Birmingham, Birmingham, B15 2TT, United Kingdom*
[7]*Ruhr Universität Bochum, Institut für Experimentalphysik 1, D-44780 Bochum, Germany*
[8]*University of Bristol, Bristol BS8 1TL, United Kingdom*
[9]*University of British Columbia, Vancouver, British Columbia, Canada V6T 1Z1*
[10]*Brunel University, Uxbridge, Middlesex UB8 3PH, United Kingdom*
[11]*Budker Institute of Nuclear Physics, Novosibirsk 630090, Russia*
[12]*University of California at Irvine, Irvine, California 92697, USA*
[13]*University of California at Los Angeles, Los Angeles, California 90024, USA*
[14]*University of California at Riverside, Riverside, California 92521, USA*
[15]*University of California at San Diego, La Jolla, California 92093, USA*
[16]*University of California at Santa Barbara, Santa Barbara, California 93106, USA*
[17]*University of California at Santa Cruz, Institute for Particle Physics, Santa Cruz, California 95064, USA*
[18]*California Institute of Technology, Pasadena, California 91125, USA*
[19]*University of Cincinnati, Cincinnati, Ohio 45221, USA*
[20]*University of Colorado, Boulder, Colorado 80309, USA*
[21]*Colorado State University, Fort Collins, Colorado 80523, USA*
[22]*Technische Universität Dortmund, Fakultät Physik, D-44221 Dortmund, Germany*
[23]*Technische Universität Dresden, Institut für Kern- und Teilchenphysik, D-01062 Dresden, Germany*
[24]*Laboratoire Leprince-Ringuet, CNRS/IN2P3, Ecole Polytechnique, F-91128 Palaiseau, France*
[25]*University of Edinburgh, Edinburgh EH9 3JZ, United Kingdom*
[26a]*INFN Sezione di Ferrara, I-44100 Ferrara, Italy*
[26b]*Dipartimento di Fisica, Università di Ferrara, I-44100 Ferrara, Italy*
[27]*INFN Laboratori Nazionali di Frascati, I-00044 Frascati, Italy*
[28a]*INFN Sezione di Genova, I-16146 Genova, Italy*
[28b]*Dipartimento di Fisica, Università di Genova, I-16146 Genova, Italy*
[29]*Harvard University, Cambridge, Massachusetts 02138, USA*
[30]*Universität Heidelberg, Physikalisches Institut, Philosophenweg 12, D-69120 Heidelberg, Germany*

[31]*Humboldt-Universität zu Berlin, Institut für Physik, Newtonstr. 15, D-12489 Berlin, Germany*

[32]*Imperial College London, London, SW7 2AZ, United Kingdom*

[33]*University of Iowa, Iowa City, Iowa 52242, USA*

[34]*Iowa State University, Ames, Iowa 50011-3160, USA*

[35]*Johns Hopkins University, Baltimore, Maryland 21218, USA*

[36]*Laboratoire de l'Accélérateur Linéaire, IN2P3/CNRS et Université Paris-Sud 11,*
Centre Scientifique d'Orsay, B. P. 34, F-91898 Orsay Cedex, France

[37]*Lawrence Livermore National Laboratory, Livermore, California 94550, USA*

[38]*University of Liverpool, Liverpool L69 7ZE, United Kingdom*

[39]*Queen Mary, University of London, London, E1 4NS, United Kingdom*

[40]*University of London, Royal Holloway and Bedford New College, Egham, Surrey TW20 0EX, United Kingdom*

[41]*University of Louisville, Louisville, Kentucky 40292, USA*

[42]*Johannes Gutenberg-Universität Mainz, Institut für Kernphysik, D-55099 Mainz, Germany*

[43]*University of Manchester, Manchester M13 9PL, United Kingdom*

[44]*University of Maryland, College Park, Maryland 20742, USA*

[45]*University of Massachusetts, Amherst, Massachusetts 01003, USA*

[46]*Massachusetts Institute of Technology, Laboratory for Nuclear Science, Cambridge, Massachusetts 02139, USA*

[47]*McGill University, Montréal, Québec, Canada H3A 2T8*

[48a]*INFN Sezione di Milano, I-20133 Milano, Italy*

[48b]*Dipartimento di Fisica, Università di Milano, I-20133 Milano, Italy*

[49]*University of Mississippi, University, Mississippi 38677, USA*

[50]*Université de Montréal, Physique des Particules, Montréal, Québec, Canada H3C 3J7*

[51]*Mount Holyoke College, South Hadley, Massachusetts 01075, USA*

[52a]*INFN Sezione di Napoli, I-80126 Napoli, Italy*

[52b]*Dipartimento di Scienze Fisiche, Università di Napoli Federico II, I-80126 Napoli, Italy*

[53]*NIKHEF, National Institute for Nuclear Physics and High Energy Physics, NL-1009 DB Amsterdam, The Netherlands*

[54]*University of Notre Dame, Notre Dame, Indiana 46556, USA*

[55]*Ohio State University, Columbus, Ohio 43210, USA*

[56]*University of Oregon, Eugene, Oregon 97403, USA*

[57a]*INFN Sezione di Padova, I-35131 Padova, Italy*

[57b]*Dipartimento di Fisica, Università di Padova, I-35131 Padova, Italy*

[58]*Laboratoire de Physique Nucléaire et de Hautes Energies, IN2P3/CNRS, Université Pierre et Marie Curie-Paris6,*
Université Denis Diderot-Paris7, F-75252 Paris, France

[59]*University of Pennsylvania, Philadelphia, Pennsylvania 19104, USA*

[60a]*INFN Sezione di Perugia, I-06100 Perugia, Italy*

[60b]*Dipartimento di Fisica, Università di Perugia, I-06100 Perugia, Italy*

[61a]*INFN Sezione di Pisa, I-56127 Pisa, Italy*

[61b]*Dipartimento di Fisica, Università di Pisa, I-56127 Pisa, Italy*

[61c]*Scuola Normale Superiore di Pisa, I-56127 Pisa, Italy*

[62]*Princeton University, Princeton, New Jersey 08544, USA*

[63a]*INFN Sezione di Roma, I-00185 Roma, Italy*

[63b]*Dipartimento di Fisica, Università di Roma La Sapienza, I-00185 Roma, Italy*

[64]*Universität Rostock, D-18051 Rostock, Germany*

[65]*Rutherford Appleton Laboratory, Chilton, Didcot, Oxon, OX11 0QX, United Kingdom*

[66]*CEA, Irfu, SPP, Centre de Saclay, F-91191 Gif-sur-Yvette, France*

[67]*University of South Carolina, Columbia, South Carolina 29208, USA*

[68]*Stanford Linear Accelerator Center, Stanford, California 94309, USA*

[69]*Stanford University, Stanford, California 94305-4060, USA*

[70]*State University of New York, Albany, New York 12222, USA*

[71]*University of Tennessee, Knoxville, Tennessee 37996, USA*

[72]*University of Texas at Austin, Austin, Texas 78712, USA*

[73]*University of Texas at Dallas, Richardson, Texas 75083, USA*

[74a]*INFN Sezione di Torino, I-10125 Torino, Italy*

[*]Deceased.

[†]Now at Temple University, Philadelphia, PA 19122, USA.

[‡]Now at Tel Aviv University, Tel Aviv, 69978, Israel.

[§]Also with Università di Perugia, Dipartimento di Fisica, Perugia, Italy.

[‖]Also with Università di Roma La Sapienza, I-00185 Roma, Italy.

[¶]Now at University of South Alabama, Mobile, AL 36688, USA

[**]Also with Università di Sassari, Sassari, Italy.

[74b]*Dipartimento di Fisica Sperimentale, Università di Torino, I-10125 Torino, Italy*
[75a]*INFN Sezione di Trieste, I-34127 Trieste, Italy*
[75b]*Dipartimento di Fisica, Università di Trieste, I-34127 Trieste, Italy*
[76]*IFIC, Universitat de Valencia-CSIC, E-46071 Valencia, Spain*
[77]*University of Victoria, Victoria, British Columbia, Canada V8W 3P6*
[78]*Department of Physics, University of Warwick, Coventry CV4 7AL, United Kingdom*
[79]*University of Wisconsin, Madison, Wisconsin 53706, USA*
(Received 15 April 2009; published 5 August 2009)

We present a study of the decays $B^0 \to D^0 K^{*0}$ and $B^0 \to \bar{D}^0 K^{*0}$ with $K^{*0} \to K^+ \pi^-$. The D^0 and the $\bar{D}^0$ mesons are reconstructed in the final states $f = K^+ \pi^-$, $K^+ \pi^- \pi^0$, $K^+ \pi^- \pi^+ \pi^-$, and their charge conjugates. Using a sample of 465×10^6 $B\bar{B}$ pairs collected with the *BABAR* detector at the PEP-II asymmetric-energy $e^+ e^-$ collider at SLAC, we measure the ratio $R_{\mathrm{ADS}} \equiv [\Gamma(\bar{B}^0 \to [f]_D \bar{K}^{*0}) + \Gamma(B^0 \to [\bar{f}]_D K^{*0})]/[\Gamma(\bar{B}^0 \to [\bar{f}]_D \bar{K}^{*0}) + \Gamma(B^0 \to [f]_D K^{*0})]$ for the three final states. We do not find significant evidence for a signal and set the following limits at 95% probability: $R_{\mathrm{ADS}}(K\pi) < 0.244$, $R_{\mathrm{ADS}}(K\pi\pi^0) < 0.181$, and $R_{\mathrm{ADS}}(K\pi\pi\pi) < 0.391$. From the combination of these three results, we find that the ratio r_S between the $b \to u$ and the $b \to c$ amplitudes lies in the range [0.07,0.41] at 95% probability.

Various methods have been proposed to determine the unitarity triangle angle γ [1–3] of the Cabibbo-Kobayashi-Maskawa (CKM) quark mixing matrix [4] using $B^- \to \tilde{D}^{(*)0} K^{(*)-}$ decays, where the symbol $\tilde{D}^{(*)0}$ indicates either a $D^{(*)0}$ or a $\bar{D}^{(*)0}$ meson. A B^- meson can decay into a $\tilde{D}^{(*)0} K^{(*)-}$ final state via a $b \to c$ or a $b \to u$ process. *CP* violation may occur due to interference between the amplitudes when the $D^{(*)0}$ and $\bar{D}^{(*)0}$ decay to the same final state. These processes are thus sensitive to $\gamma = \arg\{-V_{ub}^* V_{ud}/V_{cb}^* V_{cd}\}$. The sensitivity to γ is proportional to the ratio between the $b \to u$ and the $b \to c$ transition amplitudes (r_B), which depends on the B decay channel and needs to be determined experimentally.

In this paper we consider an alternative approach, based on neutral B mesons, which is similar to the Atwood-Dunietz-Soni (ADS) method [2] originally proposed for charged $B^- \to \tilde{D}^{(*)0} K^{(*)-}$ decays. We consider the decay channel $B^0 \to \tilde{D}^0 K^{*0}$ with $K^{*0} \to K^+ \pi^-$ [charge conjugate processes are assumed throughout the paper and K^{*0} refers to the $K^*(892)^0$]. This final state can be reached through $b \to c$ and $b \to u$ processes as shown in Fig. 1. The flavor of the B meson is identified by the charge of the kaon produced in the K^{*0} decay. The neutral D mesons are reconstructed in three final states, $f = K^+ \pi^-$, $K^+ \pi^- \pi^0$, $K^+ \pi^- \pi^+ \pi^-$. We search for $B^0 \to [\bar{f}]_D [K^+ \pi^-]_{K^{*0}}$ events, where the CKM-favored $B^0 \to \bar{D}^0 K^{*0}$ decay, followed by
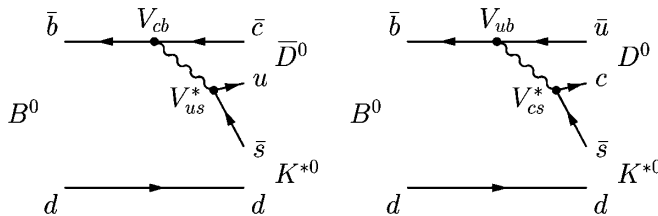
the doubly Cabibbo-suppressed $\bar{D}^0 \to \bar{f}$ decay, interferes with the CKM-suppressed $B^0 \to D^0 K^{*0}$ decay, followed by the Cabibbo-favored $D^0 \to \bar{f}$ decay. These are called "opposite-sign" events because the two kaons in the final state have opposite charges. We also reconstruct a larger sample of "same-sign" events, which mainly arise from CKM-favored $B^0 \to \bar{D}^0 K^{*0}$ decays followed by Cabibbo-favored $\bar{D}^0 \to f$ decays.

In order to reduce the systematic uncertainties, we measure ratios of decay rates

$$R_{\mathrm{ADS}} \equiv \frac{\Gamma(\bar{B}^0 \to [f]_D \bar{K}^{*0}) + \Gamma(B^0 \to [\bar{f}]_D K^{*0})}{\Gamma(\bar{B}^0 \to [\bar{f}]_D \bar{K}^{*0}) + \Gamma(B^0 \to [f]_D K^{*0})}, \quad (1)$$

$$A_{\mathrm{ADS}} \equiv \frac{\Gamma(\bar{B}^0 \to [f]_D \bar{K}^{*0}) - \Gamma(B^0 \to [\bar{f}]_D K^{*0})}{\Gamma(\bar{B}^0 \to [f]_D \bar{K}^{*0}) + \Gamma(B^0 \to [\bar{f}]_D K^{*0})}, \quad (2)$$

where R_{ADS} is the ratio between opposite- and same-sign events.

The K^{*0} resonance has a natural width (50 MeV/c^2) that is larger than the experimental resolution. This introduces a phase difference between the various amplitudes. We therefore introduce effective variables r_S, k, and δ_S [5], obtained by integrating over the region of the $B^0 \to \tilde{D}^0 K^+ \pi^-$ Dalitz plot dominated by the K^{*0} resonance, defined as follows:

$$r_S^2 \equiv \frac{\Gamma(B^0 \to D^0 K^+ \pi^-)}{\Gamma(B^0 \to \bar{D}^0 K^+ \pi^-)} = \frac{\int dp A_u^2(p)}{\int dp A_c^2(p)}, \quad (3)$$

$$k e^{i\delta_S} \equiv \frac{\int dp A_c(p) A_u(p) e^{i\delta(p)}}{\sqrt{\int dp A_c^2(p) \int dp A_u^2(p)}}. \quad (4)$$

From their definition, $0 \le k \le 1$ and $\delta_S \in [0, 2\pi]$. The amplitudes for the $b \to c$ and $b \to u$ transitions, $A_c(p)$ and $A_u(p)$, are real and positive and $\delta(p)$ is the relative strong phase. The variable p indicates the position in the

FIG. 1.   Feynman diagrams for $B^0 \to \bar{D}^0 K^{*0}$ (left, $\bar{b} \to \bar{c}$ transition) and $B^0 \to D^0 K^{*0}$ (right, $\bar{b} \to \bar{u}$ transition).

$\tilde{D}^0 K^+ \pi^-$ Dalitz plot. The parameter k accounts for contributions, in the K^{*0} mass region, of higher-mass resonances. In the case of a two-body B decay, r_S and δ_S become $r_B = A_u/A_c$ and δ_B (the strong phase difference between A_u and A_c) with $k = 1$. As shown in [6], the distribution of k can be obtained by simulation studies based on realistic models for the different resonance contributions to the decays of neutral B mesons into $\tilde{D}^0 K^{\mp} \pi^{\pm}$ final states. When considering the region in the $B^0 \to \tilde{D}^0 K^+ \pi^-$ Dalitz plane where the invariant mass of the kaon and the pion is within 48 MeV/c^2 of the nominal K^{*0} mass [7], the distribution of k is narrow, and is centered at 0.95 with a root-mean-square width of 0.03.

Because of CKM factors and the fact that both diagrams in Fig. 1 are color-suppressed, the average amplitude ratio r_S in $B^0 \to \tilde{D}^0 K^{*0}$ is expected to be of order 0.3, larger than the analogous ratio for the charged $B^- \to D^{0(*)} K^{(*)-}$ decays, which is of order 0.1 [8,9]. This implies better sensitivity to γ for the same number of events, an expectation that applies to all $B^0 \to D^{0(*)} K^{(*)0}$ decays, and that motivates the use of neutral B meson decays to determine γ. Currently, the experimental knowledge of r_S [6,10] is $r_S < 0.54$ at 95% probability.

The ratios R_{ADS} and A_{ADS} are related to r_S, γ, k, and δ_S through the following relations:

$$R_{\mathrm{ADS}} = r_S^2 + r_D^2 + 2kk_D r_S r_D \cos\gamma \cos(\delta_S + \delta_D), \quad (5)$$

$$A_{\mathrm{ADS}} = 2kk_D r_S r_D \sin\gamma \sin(\delta_S + \delta_D)/R_{\mathrm{ADS}}, \quad (6)$$

where

$$r_D^2 \equiv \frac{\Gamma(D^0 \to f)}{\Gamma(D^0 \to \bar{f})} = \frac{\int dm A_{\mathrm{DCS}}^2(m)}{\int dm A_{\mathrm{CF}}^2(m)}, \quad (7)$$

$$k_D e^{i\delta_D} \equiv \frac{\int dm A_{\mathrm{CF}}(m) A_{\mathrm{DCS}}(m) e^{i\delta(m)}}{\sqrt{\int dm A_{\mathrm{CF}}^2(m) \int dm A_{\mathrm{DCS}}^2(m)}}, \quad (8)$$

with $0 \leq k_D \leq 1$, $\delta_D \in [0, 2\pi]$, $A_{\mathrm{CF}}(m)$ and $A_{\mathrm{DCS}}(m)$ the magnitudes of the Cabibbo-favored and the doubly Cabibbo-suppressed amplitudes, $\delta(m)$ the relative strong phase, and the variable m the position in the D Dalitz plot. In the case of a two-body D decay, $k_D = 1$, r_D is the ratio between the doubly Cabibbo-suppressed and the Cabibbo-favored decay amplitudes and δ_D is the relative strong phase.

Determining r_S, γ, and δ_S from the measurements of R_{ADS} and A_{ADS}, with the factor k fixed, requires knowledge of the parameters (k_D, r_D, δ_D), which depend on the specific neutral D meson final states. The ratios r_D for the three D decay modes have been measured [7], as has the strong phase δ_D for the $K\pi$ mode [11]. In addition, experimental information is available on k_D and δ_D for the $K\pi^0$ and $K\pi\pi$ modes [12]. The smallness of the r_D ratios implies good sensitivity to r_S from a measurement of R_{ADS}. For the same reason, and since, with the present statistics, the asymmetries A_{ADS} cannot be extracted from

data, the sensitivity to γ is reduced. The aim of this analysis is therefore the measurement of r_S. In the future, good knowledge of all the r_D, k_D and δ_D parameters, and a precise measurement of the R_{ADS} ratios for the three channels, will allow γ and δ_S to be determined from this method as well.

The results presented here are obtained with 423 fb^{-1} of data collected at the $Y(4S)$ resonance with the *BABAR* detector at the PEP-II $e^+ e^-$ collider at SLAC [13], corresponding to 465×10^6 $B\bar{B}$ events. An additional "off-resonance" data sample of 41.3 fb^{-1}, collected at a center-of-mass (CM) energy 40 MeV below the $Y(4S)$ resonance, is used to study backgrounds from continuum events, $e^+ e^- \to q\bar{q}$ ($q = u$, d, s, or c). The *BABAR* detector is described elsewhere [14].

The event selection is based on studies of off-resonance data and Monte Carlo (MC) simulations of continuum and $e^+ e^- \to Y(4S) \to B\bar{B}$ events. All the selection criteria are optimized by maximizing the function $S/\sqrt{S + B}$ on opposite-sign events, where S and B are the expected numbers of opposite-sign signal and background events, respectively.

The neutral D mesons are reconstructed from a charged kaon and one or three charged pions and, in the $K\pi\pi^0$ mode, a neutral pion. The π^0 candidates are reconstructed from pairs of photon candidates, each with energy greater than 70 MeV, total energy greater than 200 MeV, and invariant mass in the interval [118, 145] MeV/c^2. The π^0 candidate's mass is subsequently constrained to its nominal value [7].

The invariant mass of the particles used to reconstruct the D is required to lie within 14 MeV/c^2 ($\simeq 1.9\sigma$), 20 MeV/c^2 ($\simeq 1.5\sigma$), and 9 MeV/c^2 ($\simeq 1.6\sigma$) of the nominal D^0 mass, for the $K\pi$, $K\pi\pi^0$, and $K\pi\pi\pi$ modes, respectively. For the $K\pi\pi\pi$ mode we also require that the tracks originate from a single vertex with a probability greater than 0.1%.

The tracks used to reconstruct the K^{*0} are constrained to originate from a common vertex and their invariant mass is required to lie within 48 MeV/c^2 of the nominal K^{*0} mass [7]. We define θ_H as the angle between the direction of flight of the K and B in the K^{*0} rest frame. The distribution of $\cos\theta_H$ is proportional to $\cos^2\theta_H$ for signal events and is expected to be flat for background events. We require $|\cos\theta_H| > 0.3$. The charged kaons used to reconstruct the $\tilde{D}^0$ and K^{*0} mesons are required to satisfy kaon identification criteria, based on Cherenkov angle and dE/dx measurements and are typically 85% efficient, depending on momentum and polar angle. Misidentification rates are at the 2% level.

The B^0 candidates are reconstructed by combining a $\tilde{D}^0$ and K^{*0} candidate, constraining them to originate from a common vertex with a probability greater than 0.1%. In forming the B, the D mass is constrained to its nominal value [7]. The distribution of the cosine of the B polar

angle with respect to the beam axis in the e^+e^- CM frame $\cos\theta_B$ is expected to be proportional to $1 - \cos^2\theta_B$. We require $|\cos\theta_B| < 0.9$. We measure two almost independent kinematic variables: the beam-energy substituted mass $m_{\mathrm{ES}} \equiv \sqrt{(E_0^{*2}/2 + \vec{p}_0 \cdot \vec{p}_B)^2/E_0^2 - p_B^2}$, and the energy difference $\Delta E \equiv E_B^* - E_0^*/2$, where E and p are energy and momentum, the subscripts B and 0 refer to the candidate B and e^+e^- system, respectively, and the asterisk denotes the e^+e^- CM frame. The distributions of m_{ES} and ΔE peak at the B mass and zero, respectively, for correctly reconstructed B mesons. The B candidates are required to have ΔE in the range $[-16, 16]$ MeV ($\simeq 1.3\sigma$), $[-20, 20]$ MeV ($\simeq 1.5\sigma$), and $[-19, 19]$ MeV ($\simeq 1.4\sigma$) for the $K\pi$, $K\pi\pi^0$, and $K\pi\pi\pi$ modes, respectively. Finally we consider events with m_{ES} in the range $[5.20, 5.29]$ GeV/c^2.

We examine background B decays that have the same final state reconstructed particles as the signal decay to identify modes with peaking structure in m_{ES} or ΔE that can potentially mimic signal events. We identify three such "peaking background" modes in the opposite-sign sample: $B^0 \to D^-[K^{*0}K^-]\pi^+$ (for $K\pi$), $B^0 \to D^-[K^{*0}K^-] \times \rho^+[\pi^+\pi^0]$ (for $K\pi\pi^0$), and $B^0 \to D^-[K^{*0}K^-] \times a_1^+[\pi^+\pi^+\pi^-]$ (for $K\pi\pi\pi$). To reduce their contribution we veto all candidates for which the invariant mass of the K^{*0} and the K^- from the D^0 lies within 6 MeV/c^2 of the nominal D^- mass.

After imposing the vetoes, the contributions of the peaking backgrounds to the $K\pi$, $K\pi\pi^0$, and $K\pi\pi\pi$ samples are predicted to be less than 0.07, 0.05, and 0.12 events, respectively, at 95% probability. Other possible sources of peaking background are $B^0 \to D^0\rho^0$ and $B^0 \to D^{*-}[D^0\pi^-]\pi^+$, which contribute to the three decay modes in both the same- and opposite-sign samples. These events could be reconstructed as signal, due to misidentification of a π as a K. We impose additional restrictions on the identification criteria of charged kaons from K^* decays to reduce the contribution of these backgrounds to a negligible level. Charmless B decays, like $B^0 \to K^{*0}K\pi$, can also contribute. The number of expected charmless background events, evaluated with data from the $\tilde{D}^0$ mass sidebands, is $N_{\mathrm{peak}} = 0.5 \pm 0.5$ (0.1 ± 1.2) in the same (opposite) sign samples.

In case of multiple D candidates (less than 1% of events), we choose the one with reconstructed $\tilde{D}^0$ mass closest to the nominal mass [7]. In the case of two B candidates reconstructed from the same $\tilde{D}^0$, we choose the candidate with the largest value of $|\cos\theta_H|$.

The overall reconstruction efficiencies for signal events are $(13.2 \pm 0.1)\%$, $(5.2 \pm 0.1)\%$, and $(6.5 \pm 0.1)\%$ for the $K\pi$, $K\pi\pi^0$, and $K\pi\pi\pi$ modes, respectively.

After applying the selection criteria described above, the remaining background is composed of continuum events and combinatorial $B\bar{B}$ events. To discriminate against the continuum background events (the dominant background

component), which, in contrast to $B\bar{B}$ events, have a jetlike shape, we use a Fisher discriminant $\mathcal{F}$ [15]. The discriminant $\mathcal{F}$ is a linear combination of four variables calculated in the CM frame. The first discriminant variable is the cosine of the angle between the B thrust axis and the thrust axis of the rest of the event. The second and third variables are $L_0 = \sum_i p_i$, and $L_2 = \sum_i p_i |\cos\theta_i|^2$, where the index i runs over all the reconstructed tracks and energy deposits in the calorimeter not associated with a track, the tracks and energy deposits used to reconstruct the B are excluded, p_i is the momentum, and θ_i is the angle with respect to the thrust axis of the B candidate. The fourth variable is $|\Delta t|$, the absolute value of the measured proper time interval between the B and $\bar{B}$ decays, calculated from the measured separation between the decay points of the B and $\bar{B}$ along the beam direction.

The coefficients of $\mathcal{F}$, chosen to maximize the separation between signal and continuum background, are determined using samples of simulated signal and continuum events and validated using off-resonance data.

The signal and background yields are extracted, separately for each channel, by maximizing the extended likelihood $\mathcal{L} = (e^{-N'})/(N!) \cdot N'^N \cdot \prod_{j=1}^N f(\mathbf{x}_j \mid \theta, N')$. Here $\mathbf{x}_j = \{m_{\mathrm{ES}}, \mathcal{F}\}$, θ is a set of parameters, N is the number of events in the selected sample, and N' is the expectation value for the total number of events. The term $f(\mathbf{x} \mid \theta, N')$ is defined as

$$f(\mathbf{x} \mid \theta, N')N'$$
$$= \frac{R_{\mathrm{ADS}}N_{DK^*}}{1 + R_{\mathrm{ADS}}} f_{\mathrm{SIG}}^{\mathrm{OS}}(\mathbf{x}|\theta_{\mathrm{SIG}}^{\mathrm{OS}}) + \frac{N_{DK^*}}{1 + R_{\mathrm{ADS}}} f_{\mathrm{SIG}}^{\mathrm{SS}}(\mathbf{x}|\theta_{\mathrm{SIG}}^{\mathrm{SS}})$$
$$+ N_{cont}^{OS} f_{cont}^{OS}(\mathbf{x}|\theta_{cont}^{OS}) + N_{cont}^{SS} f_{cont}^{SS}(\mathbf{x}|\theta_{cont}^{SS})$$
$$+ N_{B\bar{B}}^{OS} f_{B\bar{B}}^{OS}(\mathbf{x}|\theta_{B\bar{B}}^{OS}) + N_{B\bar{B}}^{SS} f_{B\bar{B}}^{SS}(\mathbf{x}|\theta_{B\bar{B}}^{SS}), \quad (9)$$

where N_{DK^*} is the total number of signal events, R_{ADS} is the ratio between opposite- and same-sign signal events, and N_{cont}^{SS}, N_{cont}^{OS}, $N_{B\bar{B}}^{SS}$, and $N_{B\bar{B}}^{OS}$ are the number of same- and opposite-sign events for continuum and $B\bar{B}$ backgrounds. The probability density functions (PDFs) f are derived from MC and are defined as the product of one-dimensional distributions of m_{ES} and $\mathcal{F}$. The m_{ES} distributions are modeled with a Gaussian for signal, and threshold functions with different parameters for the continuum and $B\bar{B}$ backgrounds. The threshold function is expressed as follows:

$$A(x) = x\sqrt{1 - \left(\frac{x}{x_0}\right)^2} \cdot e^{c(1-(x/x_0)^2)}, \quad (10)$$

where x_0 represents the maximum allowed value for the variable x described by $A(x)$ and c accounts for the shape of the distribution. The $\mathcal{F}$ distributions are modeled with Gaussians.

From the fit to data we extract N_{DK^*}, R_{ADS}, and the background yields ($N_{\mathrm{cont}}^{\mathrm{SS}}$, $N_{\mathrm{cont}}^{\mathrm{OS}}$, $N_{B\bar{B}}^{\mathrm{SS}}$, and $N_{B\bar{B}}^{\mathrm{OS}}$). We allow

TABLE I. Fit results for N_{DK^*}, R_{ADS} and the number of background events, for the three channels. The uncertainties are statistical only.

channel	$K\pi$	$K\pi\pi^0$	$K\pi\pi\pi$
N_{DK^*}	74 ± 12	146 ± 17	101 ± 17
R_{ADS}	$0.067^{+0.070}_{-0.054}$	$0.060^{+0.055}_{-0.037}$	$0.137^{+0.113}_{-0.095}$
$N^{SS}_{B\bar{B}}$	75 ± 16	265 ± 33	345 ± 35
$N^{OS}_{B\bar{B}}$	40 ± 17	215 ± 41	327 ± 48
N^{SS}_{cont}	387 ± 22	2497 ± 56	2058 ± 53
N^{OS}_{cont}	1602 ± 41	7793 ± 96	6372 ± 91

TABLE II. Systematic uncertainties ΔR_{ADS}, in units of $[10^{-2}]$, for $R^{K\pi}_{ADS}$, $R^{K\pi\pi^0}_{ADS}$, and $R^{K\pi\pi\pi}_{ADS}$.

Source	$K\pi$	$K\pi\pi^0$	$K\pi\pi\pi$
Sig. PDF	0.19	0.11	0.82
Cont. PDF	0.32	0.02	0.29
$B\bar{B}$ PDF	0.57	0.16	1.48
Peaking background	1.70	0.87	1.40
$\epsilon_{CF}/\epsilon_{DCS}$	—	0.17	0.39
Cross feed	0.04	0,05	0.02
TOTAL	1.8	0.91	2.2

the mean of the signal m_{ES} PDF and parameters of the continuum m_{ES} PDFs to float.

The fitting procedure is validated using ensembles of simulated events. A large number of pseudoexperiments is generated with probability density functions and parameters as obtained from the fit to the data. The fitting procedure is then performed on these samples. We find no bias on the number of fitted events for any of the components.

The results for N_{DK^*}, R_{ADS}, and the background yields are summarized in Table I. The total number of opposite-sign signal events in the three channels is $N^{OS}_{SIG} = 24.4^{+13.7}_{-10.9}$ (statistical uncertainty only). Projections of the fit onto the variable m_{ES} are shown in Fig. 2 for the opposite- and same-sign samples. To enhance the visibility of the signal, events are required to satisfy $\mathcal{F} > 0.5$ for $K\pi$, $\mathcal{F} > 0.7$ for $K\pi\pi^0$, and $\mathcal{F} > 1$ for $K\pi\pi\pi$. These requirements have an efficiency of about 67%, 67%, and 50% for signal and 9%, 5%, and 3% for continuum background.

The systematic uncertainties on R_{ADS} are summarized in Table II. To evaluate the contributions related to the m_{ES} and $\mathcal{F}$ PDFs, we repeat the fit by varying all the PDF parameters that are fixed in the final fit within their statistical errors, as obtained from the parametrization on simu-

lated events. To evaluate the uncertainty arising from the assumption of negligible peaking background contributions, we repeat the fit by varying the number of these events within their statistical errors. In this evaluation, we consider all the possible sources of such backgrounds, coming from charmless B decays and from B decays with a D meson in the final state, as discussed above. For the multibody D decays, the selection efficiency on same- and opposite-sign events has been confirmed to be the same, regardless of the difference in the Dalitz structure, within a relative error of 3%. Finally, a systematic uncertainty associated with cross feed between same- and opposite-sign events is evaluated from MC studies to be $(3.5 \pm 0.5)\%$, $(4.6 \pm 0.6)\%$, and $(1.9 \pm 0.4)\%$ for the $K\pi$, $K\pi\pi^0$, and $K\pi\pi\pi$ modes, respectively. The total systematic uncertainties are defined by adding the individual terms in quadrature.

The final likelihood $\mathcal{L}(R_{ADS})$ for each decay mode is obtained by convolving the likelihood returned by the fit with a Gaussian whose width equals the systematic uncertainty. Figure 3 shows $\mathcal{L}(R_{ADS})$ for all three channels, where we exclude the unphysical region $R_{ADS} \leq 0$. The
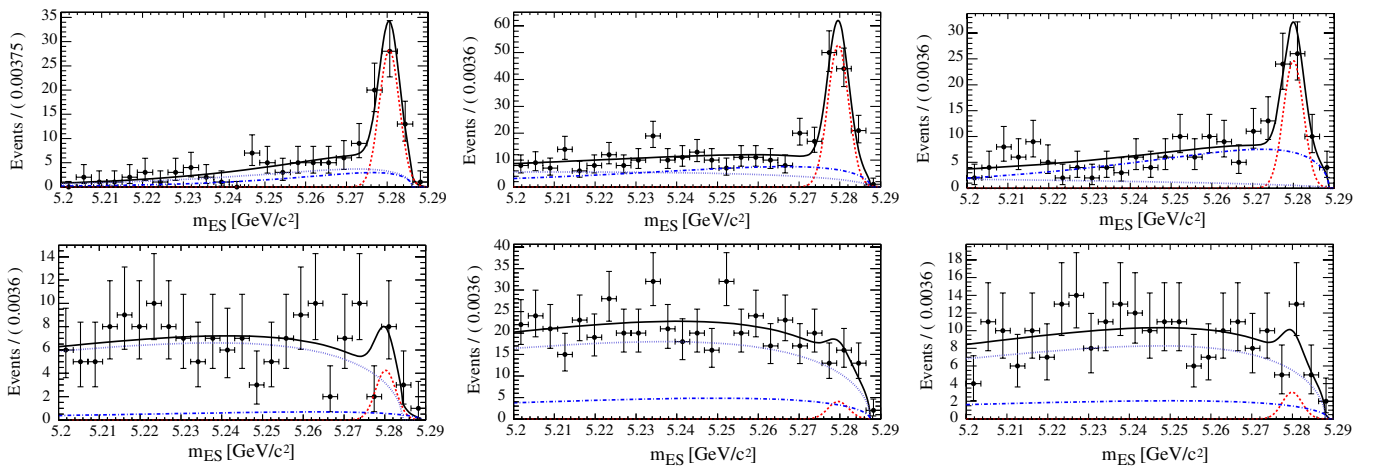

FIG. 2 (color online). Projections of the fit onto the variable m_{ES} after a cut on $\mathcal{F}$ is applied (> 0.5 for $K\pi$, >0.7 for $K\pi\pi^0$, and >1 for $K\pi\pi\pi$), to enhance the signal. The plots are shown for $K\pi$ (left), $K\pi\pi^0$ (middle), and $K\pi\pi\pi$ (right), same-sign (top) and opposite-sign (bottom) events. The points with error bars are data. The dashed, dotted, and dash-dotted lines represent the signal, continuum background, and $B\bar{B}$ background contributions, respectively. The solid line represents the sum of all the contributions.
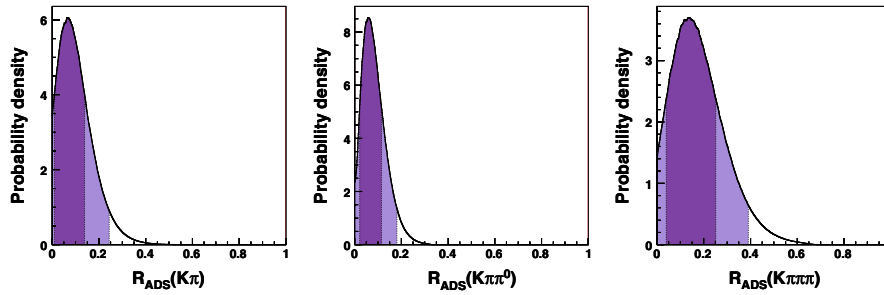
FIG. 3 (color online).   Likelihood function for $R_{ADS}(K\pi)$ (left), $R_{ADS}(K\pi\pi^0)$ (middle), and $R_{ADS}(K\pi\pi\pi)$ (right), for $R_{ADS} \geq 0$, thus excluding unphysical values. The dark and light shaded zones represent the 68% and 95% probability regions, respectively.

integral of the likelihood corresponding to $R_{ADS} < 0$ is 9.5% for $K\pi$, 15.8% for $K\pi\pi^0$, and 5.5% for $K\pi\pi\pi$. The significance of observing a signal is evaluated in each channel using the ratio $\log(\mathcal{L}_{max}/\mathcal{L}_0)$, where $\mathcal{L}_{max}$ and $\mathcal{L}_0$ are the maximum likelihood values obtained from the nominal fit and from a fit in which the signal component is fixed to zero, respectively. We observe a ratio R_{ADS} different from zero with a significance of 1.1, 1.7, and 1.4 standard deviations for the $K\pi$, $K\pi\pi^0$, and $K\pi\pi\pi$ modes, respectively. Since the measurements for the R_{ADS} ratios are not statistically significant, we calculate 95% probability limits by integrating the likelihoods, starting from $R_{ADS} = 0$. We obtain $R_{ADS}(K\pi) < 0.244$, $R_{ADS}(K\pi\pi^0) < 0.181$, and $R_{ADS}(K\pi\pi\pi) < 0.391$ at 95% probability. The overall significance of observing an R_{ADS} signal, evaluated from the combination of the three measurements, is 2.5 standard deviations.

Following a Bayesian approach, the measurements of the R_{ADS} ratios are translated into a likelihood for r_S. A large number of simulated experiments for the parameters on which R_{ADS} depends [see Eq. (5)] are performed. For each experiment, the values of $R_{ADS}(K\pi)$, $R_{ADS}(K\pi\pi^0)$, and $R_{ADS}(K\pi\pi\pi)$ are obtained and a weight $\mathcal{L}(R_{ADS}(K\pi))\mathcal{L}(R_{ADS}(K\pi\pi^0))\mathcal{L}(R_{ADS}(K\pi\pi\pi))$ is computed. In the extraction procedure to determine r_S, we use the experimental distributions for the r_D ratios, $\delta_D(K\pi)$, $k_D(K\pi\pi^0)$, $\delta_D(K\pi\pi^0)$, $k_D(K\pi\pi\pi)$, and $\delta_D(K\pi\pi\pi)$ [7,11,12]. All the remaining phases are ex-
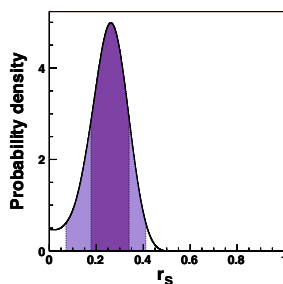
tracted from a flat distribution in the range $[0, 2\pi]$. r_S is extracted from a flat distribution in the range $[0, 1]$ and k is extracted from a Gaussian distribution with mean 0.95 and standard deviation 0.03. We obtain the likelihood $\mathcal{L}(r_S)$ shown in Fig. 4. The most probable value is $r_S = 0.26$ and we obtain, by integrating the likelihood, the following 68% and 95% probability regions:

$$r_S \in [0.18, 0.34] @ 68\% \text{probability},$$

$$r_S \in [0.07, 0.41] @ 95\% \text{probability}.$$

Given the functional dependence of R_{ADS} on r_S ($R_{ADS} \sim r_S^2$), the likelihoods corresponding to $R_{ADS} < 0$ have no effective role in the extraction of r_S. The dependence of the r_S likelihood shown in Fig. 4 on the choice of the prior distributions in the extraction procedure has been studied. While the 68% and 95% probability regions are quite stable, the likelihood shows a dependence on the choice of the prior distribution for values of r_S close to zero. For this reason, the region near zero should not be used to evaluate the significance. The significance to observe r_S different from zero corresponds to the significance for R_{ADS}, and is evaluated from the combined fit to be 2.5 standard deviations. The result obtained for r_S with the procedure described above is consistent with the result found from a direct fit to data assuming the simplified expression $R_{ADS} = r_S^2$.

In summary, we have presented a search for $b \to u$ transitions in $B^0 \to \tilde{D}^0 K^{*0}$ decays, analyzed through an ADS method. We see indications of a signal at the level of 2.5 standard deviations including systematic uncertainties. The most probable value for r_S extracted from this result is $r_S = 0.26$, where the 68% and 95% probability regions are indicated above. This result is in agreement with the phenomenological expectations from Ref. [16], and shows that the use of these decays and related ones [6] for the determination of γ is interesting in present and future facilities.

FIG. 4 (color online).   Likelihood function for r_S from the combination of the measurements of R_{ADS} obtained in the three D decay channels. The dark and light shaded zones represent the 68% and 95% probability regions, respectively.

[1] M. Gronau and D. London, Phys. Lett. B **253**, 483 (1991); M. Gronau and D. Tyler, Phys. Lett. B **265**, 172 (1991).

[2] I. Dunietz, Phys. Lett. B **270**, 75 (1991); I. Dunietz, Z. Phys. C **56**, 129 (1992); D. Atwood, G. Eilam, M. Gronau, and A. Soni, Phys. Lett. B **341**, 372 (1995); D. Atwood, I. Dunietz, and A. Soni, Phys. Rev. Lett. **78**, 3257 (1997).

[3] A. Giri, Yu. Grossman, A. Soffer, and J. Zupan, Phys. Rev. D **68**, 054018 (2003).

[4] N. Cabibbo, Phys. Rev. Lett. **10**, 531 (1963); M. Kobayashi and T. Maskawa, Prog. Theor. Phys. **49**, 652 (1973).

[5] M. Gronau, Phys. Lett. B **557**, 198 (2003).

[6] B. Aubert *et al.* (*BABAR* Collaboration), Phys. Rev. D **79**, 072003 (2009).

[7] W. M. Yao *et al.* (Particle Data Group), J. Phys. G **33**, 1 (2006).

[8] M. Bona *et al.* (UTfit Collaboration), J. High Energy Phys. 07 (2005) 028; updated results available at http://www.utfit.org/.

[9] J. Charles *et al.* (CKMfitter Collaboration), Eur. Phys. J. C **41**, 1 (2005); updated results available at http://ckmfitter.in2p3.fr.

[10] B. Aubert *et al.* (*BABAR* Collaboration), Phys. Rev. D **74**, 031101 (2006).

[11] D. M. Asner *et al.* (CLEO Collaboration), Phys. Rev. D **78**, 012001 (2008).

[12] N. Lowery *et al.* (CLEO Collaboration), arXiv:0903.4853 [Phys. Rev. Lett. (to be published)].

[13] *PEP II—An Asymmetric B Factory, Conceptual Design Report*, Report No. SLAC-418, LBL-5379, 1993.

[14] B. Aubert *et al.* (*BABAR* Collaboration), Nucl. Instrum. Methods Phys. Res., Sect. A **479**, 1 (2002).

[15] R. A. Fisher, Ann. Eugen. **7**, 179 (1936).

[16] G. Cavoto *et al.*, arXiv:hep-ph/0603019.